Applications of neutron scattering in technical catalysis: characterisation of hydrogenous species on/in unsupported and supported palladium

Peter W. Albers and Stewart F. Parker

Published version information

Citation: PW Albers and SF Parker. 'Applications of neutron scattering in technical catalysis: characterisation of hydrogenous species on/in unsupported and supported palladium.' Top Catal vol. 64, no. 9-12 (2021): 603-613.

DOI: 10.1007/s11244-021-01424-1

Applications of Neutron Scattering in Technical Catalysis:

Characterisation of Hydrogenous Species on/in Unsupported and Supported Palladium

Peter W. Albers [a] (ORCID 0000-0001-9564-1713)

and Stewart F. Parker [b] (ORCID 0000-0002-3228-2570)

a. Evonik Operations GmbH, Rodenbacher Chaussee 4, D-63457 Hanau-Wolfgang, Germany, (now retired) peterwalbers@web.de

b. ISIS Facility, STFC Rutherford Appleton Laboratory, Chilton, Didcot, OX11 0QX, UK, stewart.parker@stfc.ac.uk

Abstract

Recent results from inelastic neutron scattering (INS) measurements are reviewed that show the synergy between research on hydrogen adsorption/absorption on/in catalysts and chemical engineering. The proton dynamics of catalysts for large scale reactor technology are compared. The focus is the identification and quantification of hydrogenous species on and inside fresh, hydrogenated and dehydrogenated palladium black and supported palladium catalysts of different particle size, type of support and, therefore, morphology. INS studies of in-situ hydrogenation/ dehydrogenation of catalysts of 25 – 60 g size per sample are carried out in stainless steel cans as a function of varying hydrogen pressures. Differences in hysteresis effects in retaining hydrogen inside the catalyst in desorption from palladium hydrides and hydrogen bonding in adsorption sites in varying particle morphologies on different supports were evaluated. This aids the understanding of hydrogen/palladium interactions in catalytic processes with varying local hydrogen partial pressure, e.g. in loop reactors. The importance of the measured on-top Pd-H site in catalytic hydrogenation reactions is discussed together with previous INS results on the degree of deactivation of a technical catalyst by molecular blocking of the on-top site.

1. Introduction

From an industrial point of view neutron scattering can be highly attractive for studies of catalysts and materials of catalytic relevance, carbonaceous deposits, corrosion products and many others. Bulk quantities of material are probed non-destructively: depending on the specific morphology, density and dispersion of catalyst components sample sizes up to the 10 or even 100 g scale can be characterised in one single neutron scattering experiment with appropriate sample cans and experimental design of (*e.g.* Fig. 2 in Ref. [1] p.286). Under some conditions, such quantities may correspond to the catalyst inventory of cubic meters of reaction volume. Information of direct macroscopic relevance is obtained. The choice of sample size and measuring conditions determined in advance of the measurements together with the usual

set of previous catalyst characterization techniques, as outlined for Pt,Ru/C fuel cell catalysts in Ref. [2, p.948-9] can be crucial.

A compilation of published results from utilizing neutron scattering in the chemical industry is given in Tables S1 (catalysts/focus of investigation) and S2 (references) in the electronic supplementary information (ESI). Such activities are driven both by the long term explorative research strategy and also by time-critical demands biased by trouble-shooting jobs in everyday business. The proton dynamics of commercial and proprietary in-house materials was probed. The systems studied include various Pd, Pt, Ni based unsupported and carbon or silica supported catalysts., Other studies investigated changing a catalyst's selectivity and hydrogen storage capacity at the nanoscale by controlled poisoning by lead, as in the Lindlar catalyst ($PdPb/CaCO_3$), or by adjusting and fine-tuning a catalyst's nano-morphology. The fine structure of Pearlman's catalyst, ("$Pd(OH)_2$"/C), preferential product isomer adsorption during the Heck reaction to stilbenes, catalyst coking and phenomena of catalyst deactivation in large scale plants over time by irregular und unexpected surface blocking with molecular species were all studied (Tables S1 and S2).

During such activities it became clear that there are still unexploited potentials and synergies between chemical engineering and research on hydrogen on/in metals and hydrogen storage technology to be generated and supported by neutron scattering.

The unique hydrogen sensitivity of inelastic neutron scattering (INS) has been used for decades to study the interactions and site occupation in hydrogen storage materials ([3-6] and literature cited therein), in metals as well as alloys or intermetallic compounds and others. Due to the high hydrogen absorption capability of palladium very detailed information on the interactions with hydrogenous species is available by INS and sorption measurements [7-9].

Since the first neutron experiments in the 1950's, *ca*. 60 years of work has resulted in an improvement in neutron flux (or brightness) by a factor of about 10^2, for comparison, synchrotron radiation brightness has increased by *ca*. 10^{12}. It is widely recognized that neutron scattering will always be a flux limited technique. To partially compensate for this, there has been much work on efficient transport of neutrons by the development of neutron guides, major enhancements of detector size and efficiency, together with developments in spectrometer design. The complementary use of indirect and direct geometry instruments [10,11] provides an effective means for studying industrial catalysts of realistic composition. This has enabled us to utilize INS for studies in technical catalysis (Table S1 in the ESI), since measurements at lower metal concentrations and hydrogen level became possible. This will be illustrated here by reviewing and comparing data and conclusions on fresh and hydrogenated palladium catalysts [12,13].

For various chemical processes and in large scale plants palladium-based catalysts are used for hydrogenation reactions e.g. nitrobenzenes to anilines [14-17] and the synthesis of hydrogen peroxide [18-21] where both unsupported and supported catalysts are used.

The hydrogen concentrations in a reaction system such as a continuous loop reactor [22-24] may vary locally and/or over time of synthesis, depending on reactor technology and operation conditions, between hydrogen feed station, throughout components such as a loop reactor, heat

exchanger, catalyst filter, product separation and off-gas unit [e.g. Fig. 7 in 22]. Changes or variations of the local hydrogen concentrations and partial pressures in gas, liquid and solid phase in a macroscopic reactor can strongly affect the catalyst's activity, selectivity and physical properties: "In many cases a minimum concentration of dissolved hydrogen in the liquid in contact with the solid catalyst is needed" [25]. For the hydrogenation of nitroaromatics it was shown that the choice of solvent plus Pd-particle size influences turnover frequency [26]. With respect to the hydrogen storage capacity of palladium the question arises as to what extent a hydrogen carrier function on, and inside of, the solid catalyst throughout the reaction system may contribute to activity and selectivity in a catalytic process.

Understanding the impact of decreasing the size of precious metal entities to the nanoscale on the surface-hydrogen binding states and the overall hydrogen storage capability in the different hydride phases inside a finely dispersed palladium catalyst is challenging. Palladium powders, such as various qualities of palladium black, or nanometer-size supported palladium particles, compared in Figure 1, show differences in hydrogen absorption properties. Detailed investigations on changes of the hydrogen/palladium phase diagram of compact palladium or palladium black [9] and various nano-sized particles [27] including α- and β-hydride phase, width of the two-phase region and relative amounts of α-hydride phase at decreasing particle size were reported.

Hydrogen interactions with finely divided supported precious metal catalysts and the importance and implications of hydrogen storage in nanosized precious metal catalysts for large scale technical syntheses are still largely unexplored. For palladium catalysts operating (e.g.) in loop reactors [22,23] or others, the question arises how much surface-hydrogen and "bulk"-hydrogen can be available adsorbed or stored on/in Pd-catalysts at realistic hydrogen pressures and is there a hydrogen storage/hydrogen carrier function of the (*e.g.*) palladium catalyst during operation and/or passing through a reactor ? Can there be differences in hysteresis effects in hydrogen absorption/desorption from varying bonding modes of hydrogen in-process for fresh and operating catalysts? Here synergies between fundamental hydrogen-in-metals research and industrial reactor technology in chemical engineering are available.

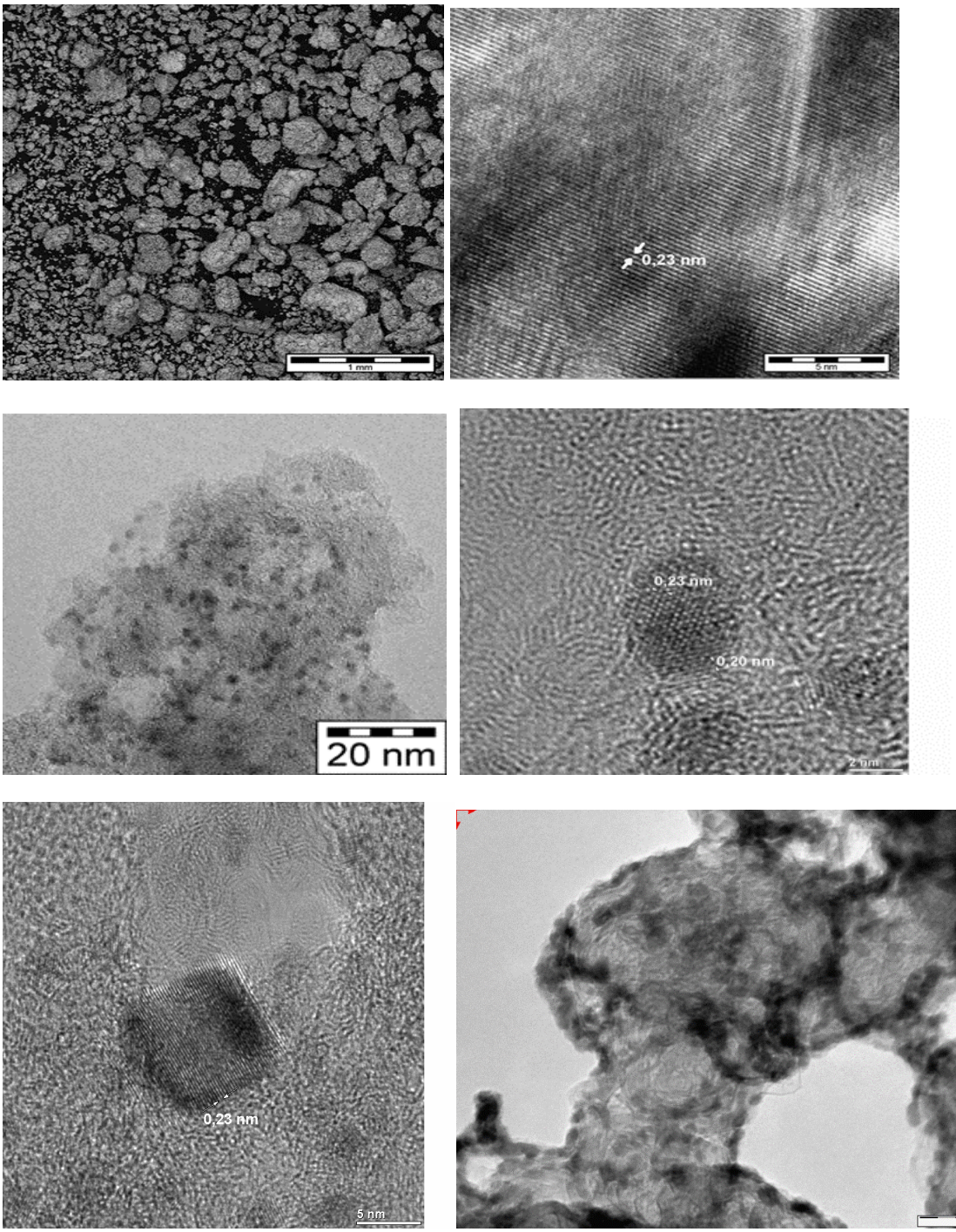

Fig. 1 Comparison of the morphology of some grades of palladium catalysts. Top: commercial palladium black as received, top left: scanning electron microscopy revealing a polydisperse variety of granules, agglomerates/aggregates, top right: transmission electron microscopy revealing the extended size and long range crystalline order of a metallic primary crystallite. Middle: Pd/C catalyst of mostly isolated primary particles of Pd well-dispersed over the para-crystalline carbon support that shows turbostratic disorder; the ca. 2-5 nm sized primary Pd-particles (middle right) resemble cubo-octahedral geometry whereas ca. 10 nm sized Pd-particles (bottom left) appear cube shaped; in a Pd on carbon black (bottom right) catalyst edge decoration of the precious metal by deposition onto the carbon support and growth to Pd aggregates/agglomerates is observed. These morphological differences are of relevance for variation of hydrogen sorption isotherms and storage.

Figure 1 illustrates the different morphologies of industrial palladium catalysts, ranging from larger crystallites, intergrown aggregates of primary particles to nano-sized isolated primary particles. Different diameters and shapes translate into differences in long- and short range-order which can explain variations in the α-/β-hydride phase formation and ratio:

- Differences found in hydrogen absorption studies [9, 27-30] for larger and isolated small Pd particles with different average primary particle size

- Differences in the width and position of the α-/β-phase transition region [27-30] due to varying long-range phase coherence, the latter being of relevance for the hydride phase transition [31,32]

- Results from computational studies on long-range attractive forces and short-range repulsive forces and the phase stability in palladium hydrides [33]

Results and discussion

Fig. 2, top and Fig. 3, top show the INS spectra of as received Pd black and a Pd/C catalysts respectively, after evacuation in the INS can, but without any hydrogenation/reduction treatment. Both spectra are dominated by Pd-OH vibrations. The analysis of the bending, wagging and stretching modes of the surface hydroxyls supplements the corresponding data from X-ray photoelectron spectroscopy (Fig. 3, bottom). This is used to evaluate the degree of surface oxidation of the Pd by a qualitative or semi-quantitative check of the presence of reduced or oxidized Pd-species: at about 334.9 eV and more Pd (depending on metal dispersion), sub-stoichiometric surface species PdO_x $x<1$ at ca. 335-336 eV, and nominally, 336.3 eV PdO, 337.9 eV PdO_2 [34]. A more detailed assignment in the region of ca. 335-337 eV seems to be complicated by interference from proton-related signal contributions of hydrogenous palladium/oxygen surface species such as $PdO_x(OH)_y$ / $Pd(OH)_z$ whose presence and influence can be investigated in more detail by INS. This was already demonstrated by previous work on hydrous palladium oxide [35] and on the fine structure of Pearlman's catalyst revealing the presence of a layered C/PdO/OH/H_2O structure rather than a completely stoichiometric $Pd(OH)_2$/C [36].

More detailed knowledge of the hydroxyl/water/oxides to palladium balance present at a fresh catalyst surface is important with respect to de-wetting treatment of fresh catalysts to fine-tune dispersibility, floating properties, separation and filtration during operation in various process applications.

A subsequent series of INS spectra (Fig. 2-5) reveal how efficiently after hydrogenation/dehydrogenation cycles at moderate hydrogen pressures (700-1500 mbar at room temperature, [9,37]) the surface hydroxyls and traces of residual water were removed for the case of Pd, whereas enforced treatments at higher pressure and temperature are necessary for Ni [38] and especially to dehydroxylate and reduce [39] finely divided Co-particles to form Co-H [40].

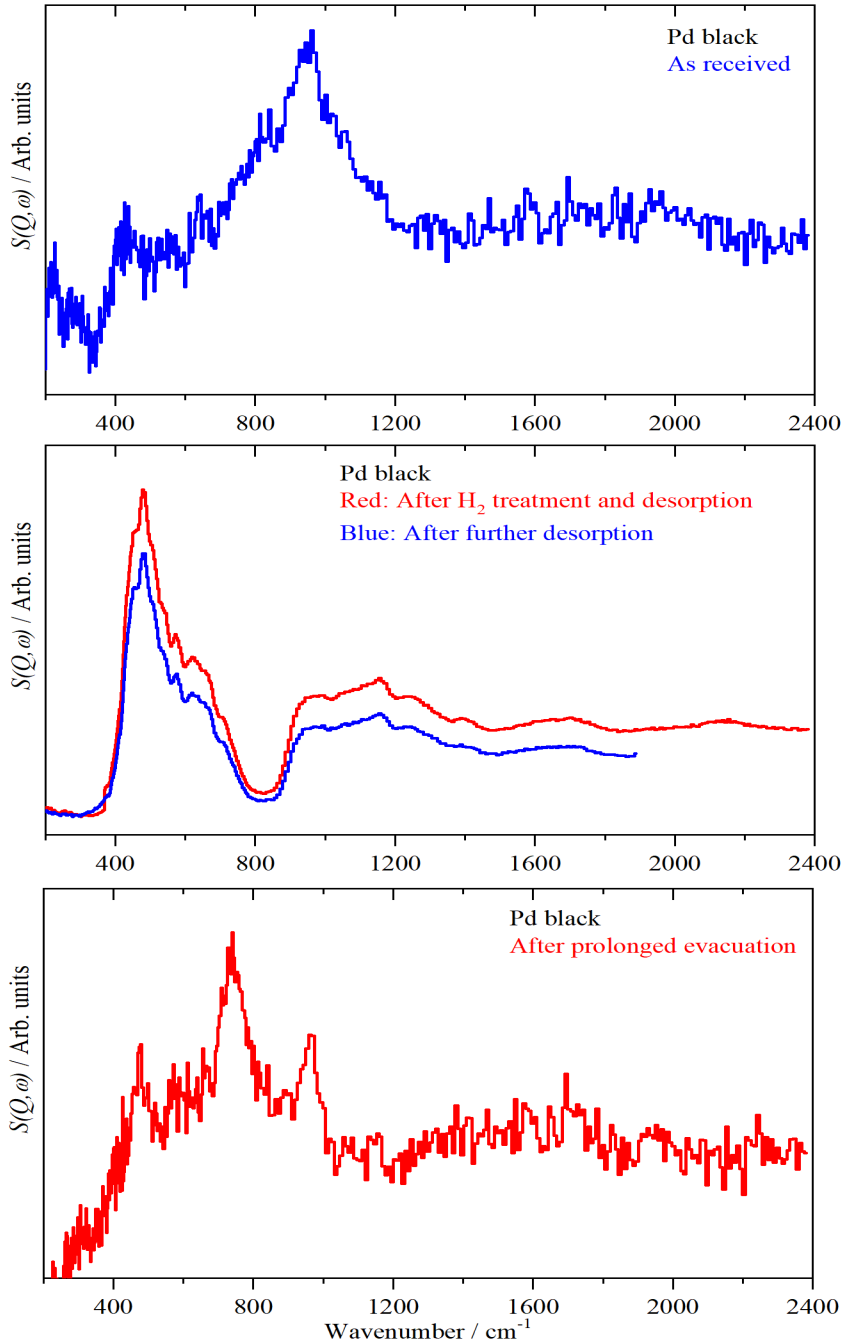

Fig. 2 IINS spectra of 60 g of Pd black recorded on Lagrange at the ILL/Grenoble/France, top: fresh, as received and evacuated (215 cm^{-1} Pd-OH-Pd wagging mode, 425 cm^{-1} Pd-OH-Pd stretching, 950 cm^{-1} Pd-O-H bending, 1870 cm^{-1} 1st overtone), middle: after H_2 loading/unloading/loading cycles (485 cm^{-1} and asymmetric shoulder around 640 cm^{-1} β-PdH_x, 574 cm^{-1} α-PdH_y, 1050 1st overtone), bottom: after prolonged hydrogen desorption and evacuation (470 cm^{-1} sub-surface hydrogen/β-PdH, 740 and 970 cm^{-1} Pd/H in C_{3v} site). Reproduced from [12].

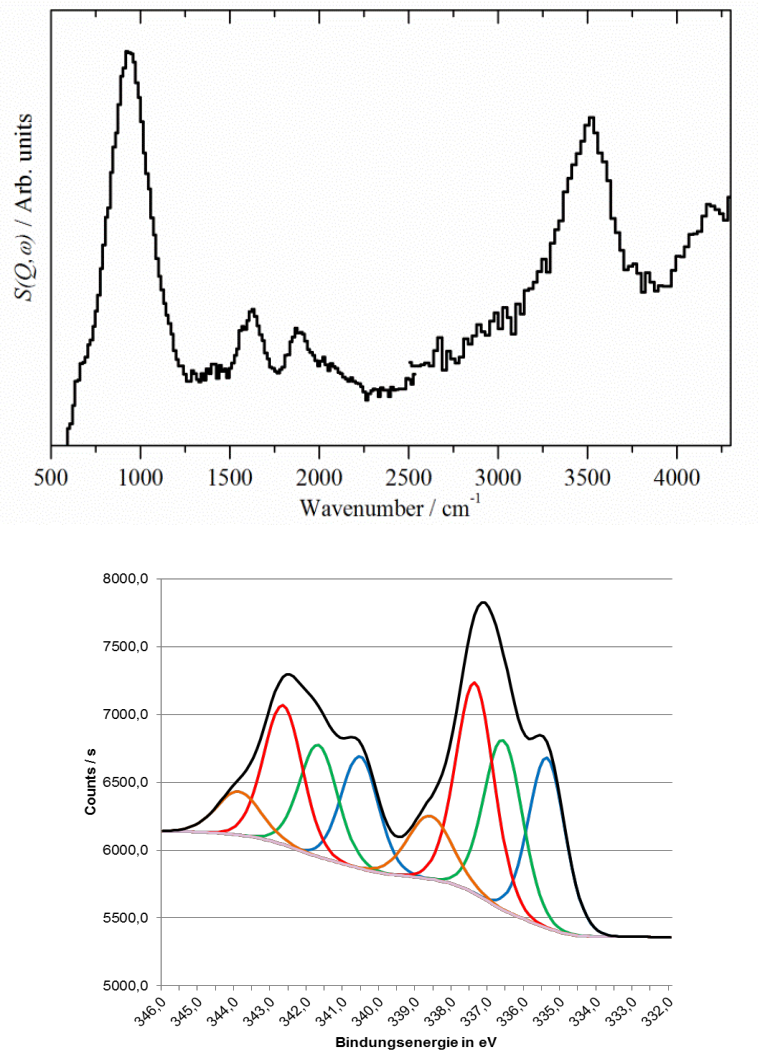

Fig. 3 top: IINS spectrum of 25 g of 20%Pd/carbon black catalyst, fresh, as received, recorded on MERLIN at ISIS/Chilton/UK, Pd-O-H bending mode and first overtone 940 and 1880 cm^{-1}, broad O-H stretching mode (surface hydroxyls) at 3520 cm^{-1}, shoulder at ca. 3400 cm^{-1} (water). Bottom: Gaussian/Lorentzian line shape approximation of XPS spectral region $Pd3d_{3/2}$ and $3d_{5/2}$. Top part reproduced from [12] under a Creative Commons Attribution Unported License 3.0 (CC BY).

The stretching mode of the Pd-H on-top species is shown in Fig. 4. Since both, the β-PdH_x signal, overtones and that of the on-top site at 2150 cm^{-1} are available from one single spectrum, a rough estimate of the ratio of hydrogen stored inside and located on the surface of the supported palladium particles was possible: surface : bulk-hydrogen of 1 : 8, note that this includes an unknown contribution from hydrogen in high coordination sites at the surface. This numerical estimation also illustrates the hydrogen storage potential function present in the interior of the small supported particles. These are present largely as aggregates leading to long range order (see also Fig. 5, top right) which is essential for β-phase hydride formation.

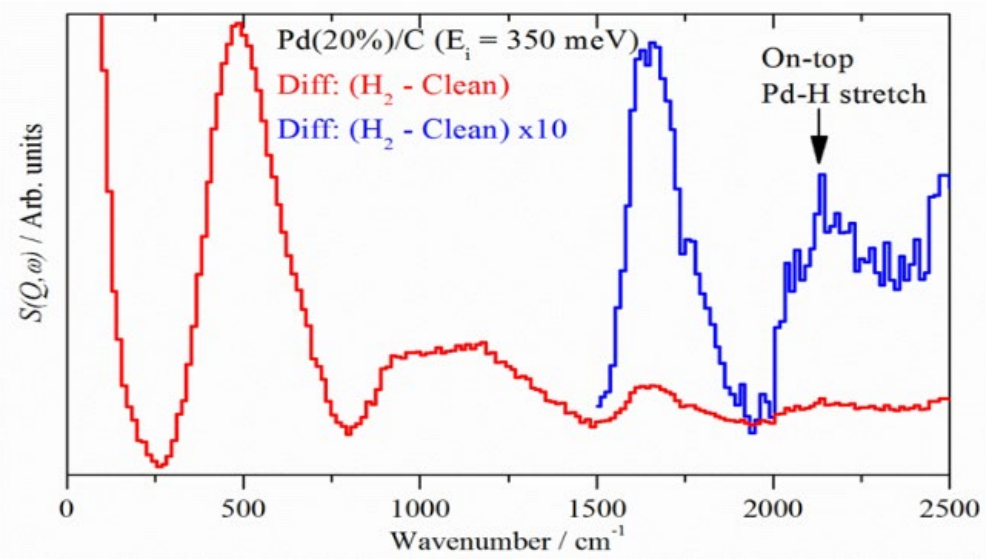

Fig. 4 25 g of 20% Pd/carbon black catalyst after removal of surface-hydroxyls (Fig. 3 top), by H_2 loading/unloading/loading cycles recorded under 700 mbar hydrogen pressure to generate β-$PdH_{0.7}$ as determined by neutron diffraction on SANDALS. Detection of β-palladium hydride transitions at 400-600 cm^{-1} (0 → 1), 800-1400 cm^{-1} (0 → 2), 1500-1800 cm^{-1} (0 → 3), and 2150 cm^{-1} on-top Pd-H stretch mode. Reproduced from [13] under a Creative Commons Attribution Unported License 3.0 (CC BY).

Figs. 5 and 6 show changes of proton dynamics and residual hydrogen storage of catalysts after hydrogenation and dehydrogenation at decreasing hydrogen equilibrium pressure. Fig. 6 shows significant differences after hydrogen desorption treatment under comparable conditions: residual β-phase, subsurface hydrogen 470 cm^{-1}, ca. 560 α-PdH, H in C_{3v} sites at the surface 740/820, 970 cm^{-1} (Pd-H stretch). Evaluation of the hydrogenous scattering from the INS data enables quantification of the differences that are the result of changes in primary particle size. The choice of support, together with precious metal deposition technique, determines whether the catalyst predominantly consists of isolated primary particles (as on activated carbon) or aggregates/agglomerates (as on carbon black). Subsequent thermal modification can simultaneously cause break-up of aggregates into primary entities and particle growth, as shown in Table 1. The structural differences translate into differing hydrogen storage capability and also affect to what extent palladium hydrides were formed or could be modified by dehydrogenation treatments. Furthermore, the presence of hysteresis effects in hydrogen desorption or trapping in the catalyst can be studied (Fig. 5 middle and bottom).

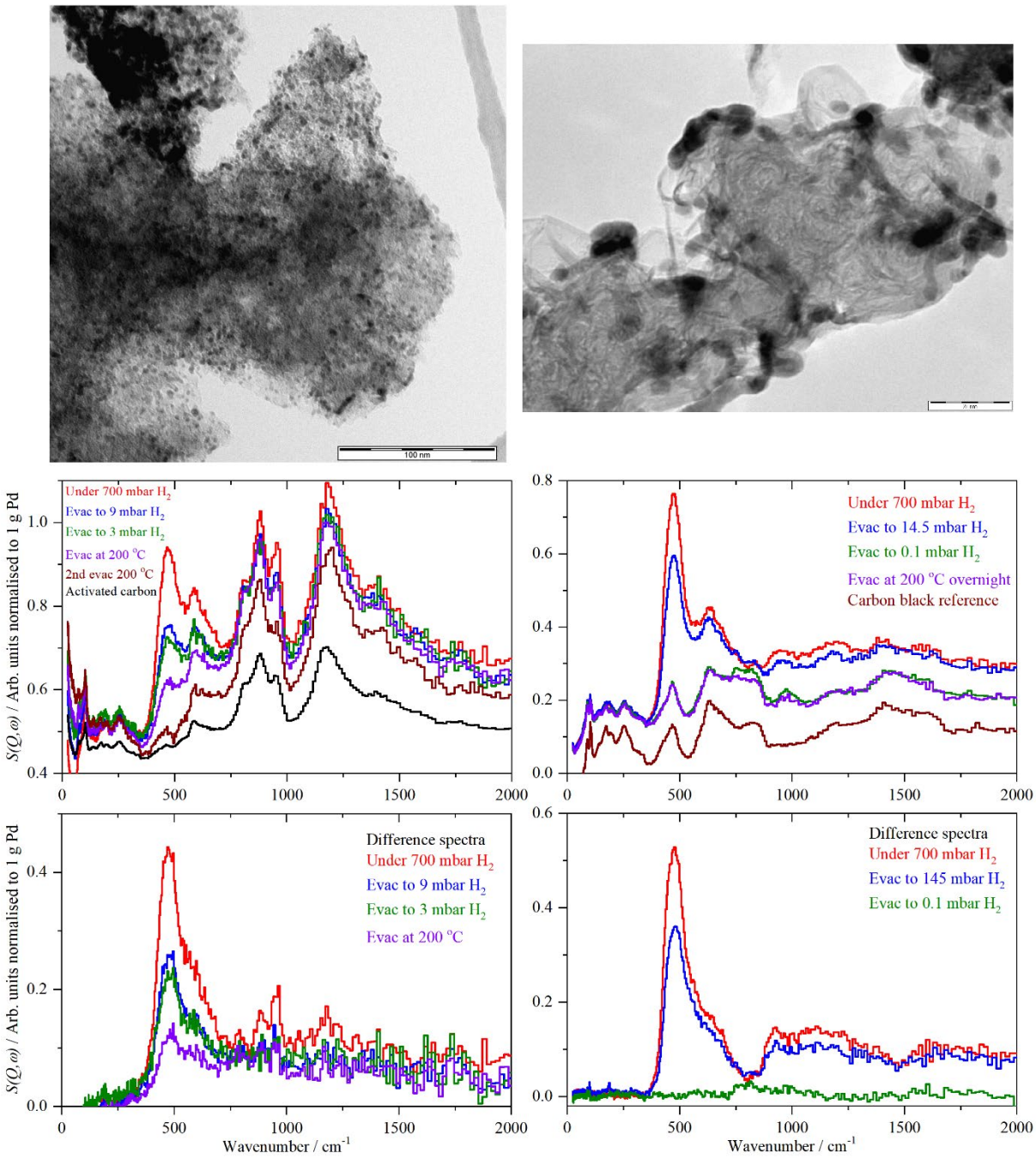

Fig. 5 25 g 20%Pd/C catalysts. Top: TEM micrographs show isolated primary particles of Pd on activated carbon (left) and intergrown aggregates of primary particles plus isolated primary particles of palladium on carbon black (right). Middle and bottom: IINS spectra recorded after in-situ hydrogenation in the can recorded under similar hydrogen pressures (ca. 700 →5 10 → 1 mbar). Middle: as recorded normalized to weight. Bottom: After background subtraction (supporting carbon and can) to highlight the hydrogenous scattering. Reproduced from [13] under a Creative Commons Attribution Unported License 3.0 (CC BY).

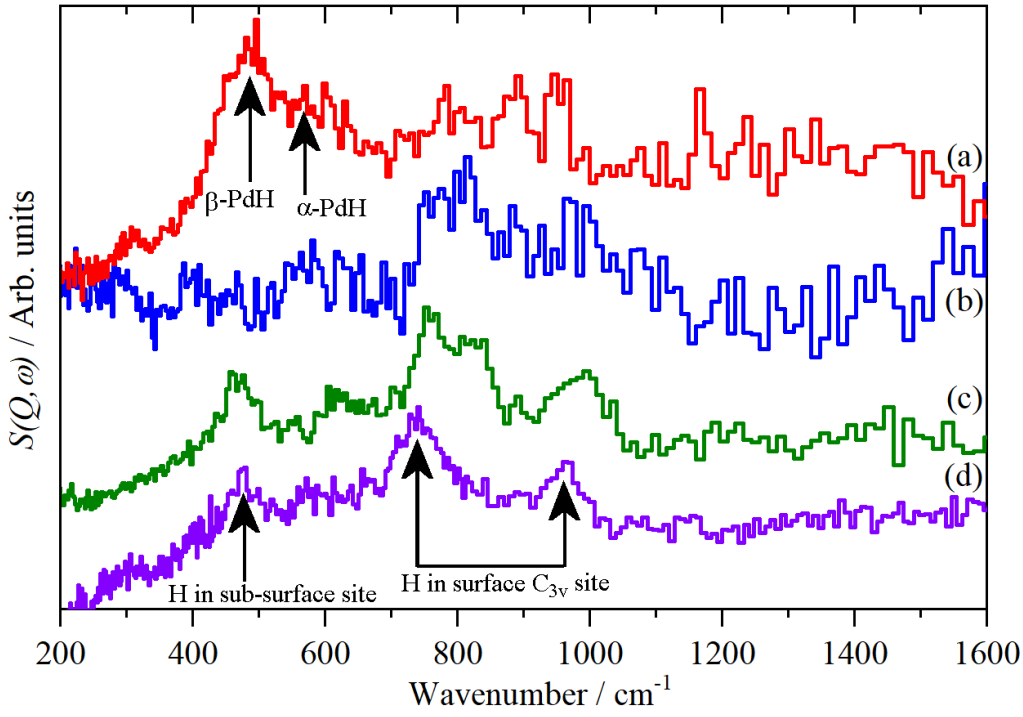

Fig. 6 INS spectra of catalysts of different average primary particle size (bound in aggregates or isolated), (a) red Pd/AC 3.6 nm, (b) blue Pd/CB 2.4 nm, (c) green Pd/CB annealed at 300°C for de-agglomeration/ de-aggregation plus particle growth Pd/CB 6.7 nm and (d) violet Pd black (see Fig. 1) Reproduced from [13] under a Creative Commons Attribution Unported License 3.0 (CC BY).

Table 1. Integrated area (arbitrary units) of the PdH region (350 – 800 cm^{-1}) of the INS spectra in order of increasing average primary particle size DN. The data for the Pd/AC and Pd/CB samples are for the spectra shown in the bottom panels of Fig. 5. The spectra of the Pd/CB 300° and Pd/CB 400° samples are shown in [13] and the ESI to [13], respectively.

Catalyst† / dominating morphology	TEM PP DN (nm)	IINS area ca. 700 mbar H_2	IINS area ca. 10 mbar H_2	IINS area ca. 1 mbar H_2	IINS area ΔT-degas
Pd/CB AGG/(PP)	2.40	78.87	55.14	6.84	
Pd/AC PP	3.58	59.87	32.97	29.66	12.28
Pd/CB 300° PP/AGG	6.73	99.00	74.66	18.68	
Pd/CB 400° PP	7.74	77.97	23.15	9.06	9.00

†Catalysts: Pd on activated carbon (AC), carbon black (CB), morphology (AGG aggregates, PP primary particles) average primary particle size (isolated primaries and/or aggregated primaries).

This information provides a link to large scale chemical engineering. In the case of palladium, the α-/β-phase transition region and the corresponding hydrogen storage window at constant

hydrogen equilibrium pressure, below 750 mbar, are very broad [9]. The β-hydride phase is formed and saturated at pressures well below the 750 mbar hydrogen pressure (ca. 10-20 mbar plateau region) used in our measurements. Further, the isotherms of Pd black and supported Pd show a very steep increase with pressure once the β-phase is obtained up to 1 to 100 bar and more. Very similar isotherms are obtained at both 20° and 80° C [Fig. 3.4 in Ref. [9] and Fig. 7 in Ref. 37].

This holds for the steep β-phase branch for coarse as well as for finely divided palladium. The consequence is that our measurements of the relative amounts of β-phase hydride present in the catalysts inside the INS cans at 20°C and 750-1500 mbar are essentially those that would be obtained at higher pressure (ca. 10-100 bar) hydrogen pressure and enhanced temperature (80-200°C) and hence are directly relevant to industrial catalyst operation.

A striking difference in catalytic activity and selectivity could be the result of differences in the relative proportions in α- and β-hydride phase (Fig. 6) and the changes of the width of the two-phase region, with decreasing Pd-particle size and changes between isolated and aggregated primary structures (Fig. 1, Fig. 5 top).

Fig. 7 summarises the states of hydrogen on/in palladium as a function of hydrogen content: at the lowest hydrogen content only the surface threefold sites are occupied, the sub-surface site is then filled, migration of this into the bulk generates α-PdH and further hydrogen results in formation of β-PdH with the on-top sites occupied. This loading process is reversible (Figure 5 and Table 1) to different extents in hydrogenation/dehydrogenation cycles as occurring (*e.g.*) in loop processes. These hydrogenous species may appear in/on the Pd-black as well as Pd supported on activated carbon or carbon black to a varying degree in the catalyst separation / filtration unit, because of potential residues of hydrogen dissolved in the liquid or residual gas bubbles.

From Figure 7, bottom, on the on-top Pd-H site the question arises about the impact of competition on this exposed position with larger molecular entities in potential catalyst deactivation.

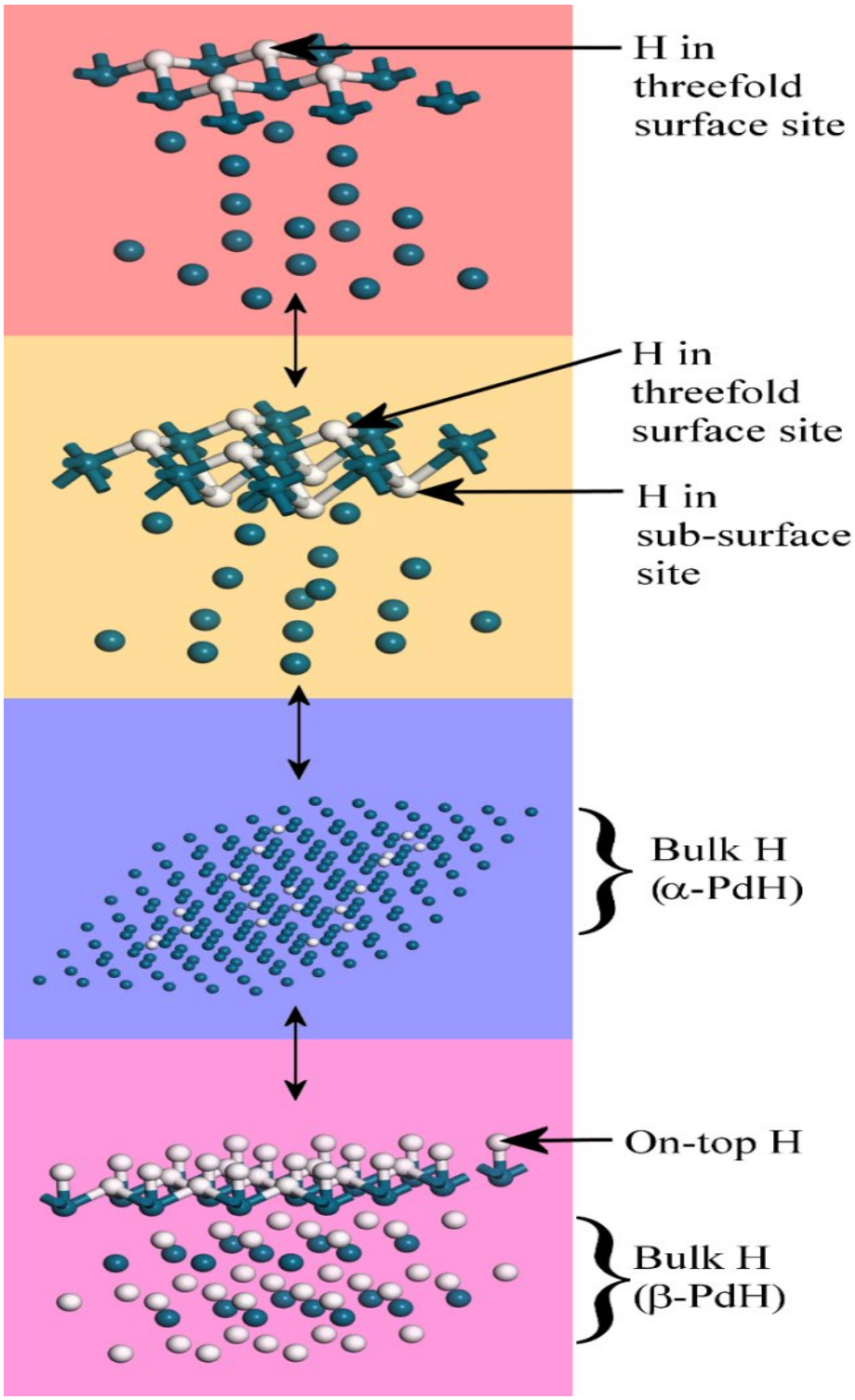

Fig. 7 Schematic representation of the Pd/H species detected by in-situ INS measurements with increasing hydrogen pressure. Reproduced from [13] under a Creative Commons Attribution Unported License 3.0 (CC BY).

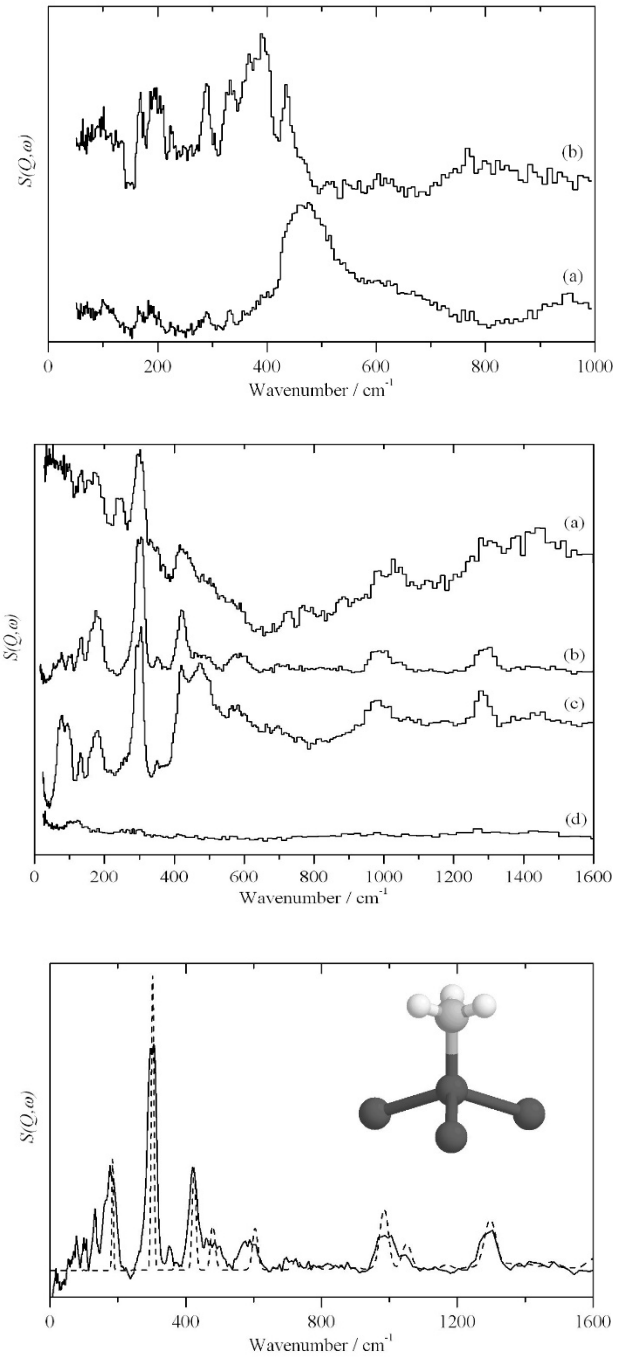

Fig. 8 Biography of a deactivation phenomenon in a large scale plant over time. Top: a) catalyst measured under hydrogen, detection of the presence of β-PdH, b) after pumping down, non-extractable molecular species at the catalyst surface are detected. Middle: a) largely deactivated catalyst with adherent organics, b) after extraction of the organics, non-extractable simple molecular species remain at the surface, c) as b) after hydrogenation, in-situ in the INS can, β-PdH is formed, the molecular species remain as indicated by very sharp peaks as a signature of a simple and/or symmetric molecular structure, d) directly comparable, highly active catalyst without any deactivation. Bottom: assignment of the surface species as CH_3 in on-top-bonding. Adsorption of H as Pd-H on top and adsorption of reactants is hampered. Formation of β-phase palladium hydride is hindered, but possible (middle c, top a). Top and middle: reproduced from [43] with permission from Elsevier, bottom: reproduced from [41] with permission from The Royal Society of Chemistry.

The importance of the on-top site in technical catalysis was illustrated by a long-term deactivation phenomenon in a large-scale hydrogenation plant [41-43], Fig. 8. Sample sizes in the 20-40 g scale were investigated, both before and after solvent extraction. Over time. a palladium catalyst that was operating in a technical loop reactor, became contaminated by strongly adherent, non-extractable surface species, in parallel, the overall catalytic activity was progressively decreased. The drop in activity correlated quantitatively with the presence, and normalized intensity of, a narrow INS band at 302 cm^{-1} which could be assigned to the torsion of a methyl group having C_{3v} symmetry, bound to the on-top site on Pd(111) facets. The CH_3 torsion in the residual adherent organic liquid traces was observed at ca. 240 cm^{-1} in the weakly adsorbed molecules. This mode was completely absent after liquid phase solvent extraction of the deactivated catalyst, whereas the 302 cm^{-1} signal remained unchanged [43], Fig. 8, trace a, b therein]. The adsorption of sp^2 polycyclic aromatic reactants at the Pd surface for selective hydrogenation was prevented by the chemically bound sp^3 type molecular species. However, hydrogen uptake into the octahedral sites [7,8] of the palladium (as shown by the β-hydride band at about 464 cm^{-1}, 1st overtone 930 cm^{-1}) and the release of hydrogen by the catalyst was still possible, even in the presence of a bonded molecular precursor species [43], Fig. 8 trace c therein], albeit, at a reduced level of hydrogen storage capacity. The stability of Pd-CH_3 is, for example, in line with the frustration of methane formation in Fischer-Tropsch catalysis [44], results of calculations on CH_x (x=0-3) on Pd(111) that CH_3 is the stable species [45], and the conclusion on the slow step in CO methanation being the reaction of methyl groups and hydrogen [46].

This finding illustrates:

- the importance of the on-top position for catalytic activity in commercial hydrogenation processes

- the effect of inhibiting hydrogen adsorption into C_{3v} surface sites by blocking with organic degradation products and the influence on the possibility of the surface to accommodate relevant amounts of on-top hydrogen

- at high hydrogen loading the existence of β-palladium hydride exhibiting very high band intensity for a fresh, active catalyst together with on-top hydrogen, Fig. 4

- the existence of β-palladium hydride exhibiting somewhat lower band intensity for a deactivated catalyst with partial surface shielding by chemically bonded small organic entities

Several influences have to be considered:

the amount of hydrogen that can be stored inside palladium, how this varies with particle size and shape and whether these are present as isolated primary particles or aggregates (Table 1) and the relative amounts of α- and β-phase hydride, which are relevant for selectivity and activity in catalytic hydrogenation [37], and the relative amounts of hydrogen bonding to surface and surface-near sites.

Conclusions

This review focused on the comparison of INS results on commercial unsupported and supported palladium catalysts as received and after cycles of hydrogenation/dehydrogenation treatments in-situ. Details of the chemical changes in the surface regions and inside the precious metal are discussed. These findings allow analogies with chemical engineering on the behaviour of catalysts operating in loop and trickle bed reactors. De-wetting and conditioning of fresh catalysts to remove hydroxyls can be studied. Changes at the adsorption sites such as the surface threefold $\rightarrow$ surface threefold + sub-surface hydrogen and the hydrogen storage and hydride formation of phase $\rightarrow$ α-PdH $\rightarrow$ β-PdH and the occupation of the Pd-H on-top site on the fully hydrogenated palladium hydride can be followed and, vice versa, the controlled dehydrogenation at different steps of partial pressure.

The importance of the Pd-H on-top site is underlined by INS results on the deactivation of technical palladium catalysts by competitive occupation with small molecular Pd-CH_3 entities bound to the on-top position. This deactivation is different to classical physical coke deposition. Adsorption of reactants for hydrogenation at the catalyst surface is hampered but the hydrogen storage function to β-palladium hydride is still possible.

Compliance with Ethical Standards

The authors have no conflicts of interest. There were no human or animal subjects involved in this research.

Acknowledgements

The STFC Rutherford Appleton Laboratory is thanked for access to the neutron beam facilities of TOSCA, MAPS, MERLIN and SANDALS. The Institut Max von Laue-Paul Langevin (ILL), Grenoble, France is thanked for access to the high flux reactor facilities (IN1 Lagrange).

References

1. Albers PW, Lennon D., Parker SF (2017) Catalysis. In: Fernandez-Alonso F, Price DL (eds), Experimental Methods in the Physical Sciences, Neutron Scattering: Applications in Chemistry, Materials Science, and Biology. vol. 49, Academic Press, UK, Oxford, pp. 281-350.

2. Ruth K, Albers P (2018) Materials for solid catalysts. In: Warlimont H, Martienssen W (eds) Springer Handbook of Materials Data 2nd Ed., Springer Nature, Switzerland, Cham, pp. 935-955.

3. Richter D, Hempelmann R, Bowman Jr. RC (1992) Dynamics of hydrogen in intermetallic compounds. In: L. Schlapbach L (ed) Hydrogen in Intermetallic Compounds II, Surface and Dynamic Properties, Applications, Topics in Applied Physics vol. 67, Springer, Berlin, Germany, pp. 97-164.

4. Ross DK (1997) Neutron scattering studies of metal-hydrogen systems. In: Wipf H (ed.) Hydrogen in Metals III: Properties and Applications Topics in Applied Physics Vol. 73, Springer, Germany, Berlin, Germany, pp. 153-214.

5. Celli M, Colognesi D, Zoppi M, (2009) Hydrogen and hydrogen-storage materials. In: Liang L, Rinaldi R, Schober H (eds) Neutron Applications in Earth, Energy and Environmental Sciences, Springer Science +Business Media, LLC, Switzerland, pp 417-438.

6. Ross DK, Roach DL (2016) Inelastic and quasi-elastic neutron scattering. In: Fritzsche H., Huot J, Fruchard D (eds) Neutron Scattering and Other Nuclear Techniques for Hydrogen in Materials, Springer International Publishing, Switzerland, pp. 245-276.

7. Drexel W, Murani A, Tocchetti D, Kley W, Sosnowska I, Ross DK (1976) The motions of hydrogen impurities in α-palladium-hydride J Phys Chem Solids 37: 1135-1139.

8. Ross DK, Martin PF, Oates WA, Khoda Bakhsh R (1979) Inelastic neutron scattering measurements of optical vibration frequency distributions in hydrogen-metal systems. Z Phys Chem 114: 221-230.

9. Wicke E., Brodowski H. (1978) Hydrogen in palladium and palladium alloys. In: Alefeld G, Völkl J (eds) Hydrogen in Metals II: Application-Oriented Properties, Topics in Applied Physics vol. 29, Springer, Germany, Berlin, pp. 73-155.

10. Parker SF, Lennon, D, Albers PW (2011) Vibrational spectroscopy with neutrons – new directions. Applied Spectroscopy 65: 1325-1341.

11. Parker SF, Ramirez-Cuesta AJ, Albers PW, Lennon D (2014) The use of direct geometry spectrometers in molecular spectroscopy. DMMII, Journal of Physics: Conference Series 554: 012004.

12. Parker SF, Adroja, D, Jimenez-Ruiz M, Tischer M, Möbus K, Wieland SD, Albers P (2016) Characterisation of the surface of freshly prepared precious metal catalysts. Phys Chem Chem Phys 18: 17196-17201.

13. Parker SF, Walker HC, Callear SK, Grünewald E, Petzold T, Wolf D, Möbus K, Adam J, Wieland SD, Jiménez-Ruiz M, Albers PW (2019) The effect of particle size, morphology and support on the formation of palladium hydride in commercial catalysts. Chem. Sci. 10: 480-489.

14. Kosak, JR (1996). Precious metal synergism in catalytic hydrogenation. In: Catalysis of Organic Reactions (Chemical Industries) Malz Jr RE (ed) Dekker, New York, pp. 31–41.

15. Booth G (2007). Nitro Compounds, Aromatic. In Ullmann's Encyclopedia of Industrial Chemistry, 7th ed., vol. 24, Wiley-VCH, Germany Weinheim, pp. 301–350.

16. Randall D, Lee S (2002) The Polyurethanes Book, John Wiley, USA, New York

17. Parker GL, Smith LK, and Baxendale IR (2016) Development of the industrial synthesis of vitamin A, Tetrahedron, 2016, **72**, 1645-1652.

18. Weigert W (1978) Wasserstoffperoxid und seine Derivate: Chemie u. Anwendungen. Hüthig-Verlag, Germany, Heidelberg.

19. Jones CW (1999) Applications of hydrogen peroxide and derivatives. RSC Clean Technology Monographs, Royal Society of Chemistry, Cambridge, 1999.

20. Chen Q (2008) Development of an anthraquinone process for the production of hydrogen peroxide in a trickle bed reactor—From bench scale to industrial scale. Chem Eng Proc: Proc Intensification 47: 787-792.

21. Goor G, Glenneberg J, Jacobi S (2012) Hydrogen peroxide. In: Ullmanns's Encyclopedia of Industrial Chemistry, 7th ed., vol. 18, Wiley-VCH, Weinheim, pp. 393-427.

22. Duveen RF (1998) High performance gas-liquid reaction technology. HH Technology Corp., Sissach, Switzerland, http://www.hhcorp.net/PDF/Rene_High_Performance.pdf. Accessed 28 January 2021.

23. Warmeling H, Behr A, Vorholt AJ (2016) Jet loop reactors as a versatile reactor set up – Intensifying catalytic reactions: A review. Chem Eng Sci 140: 229-248.

24. Wood J (2016) Three-phase catalytic reactors for hydrogenation and oxidation reactions. Phys Sci Rev 1: 20150019.

25. Satterfield CN (1975) Trickle-Bed Reactors. AIChE Journal 21: 209-228.

26. Gelder EA, Jackson SD, Lok CM (2002) A study of nitrobenzene hydrogenation over palladium/carbon catalysts. Catal Lett 84: 205-208.

27. Pundt A, Suleiman M, Bähtz C, Reetz MT, Kirchheim R, Jisrawi NM (2004) hydrogen and Pd-clusters. Mat Sci Eng B 108**:** 19-23.

28. Pundt A, Sachs C, Winter M, Reetz MT, Frisch D, Kirchheim R (1999) Hydrogen sorption in elastically soft stabilized Pd-clusters. J Alloys Compounds 293-295: 480-483.

29. Sachs C, Pundt A, Kirchheim R, Winter M, Reetz MT, Frisch D (2001) Solubility of hydrogen in single-sized palladium clusters. Phys Rev B 64**:** 075408.

30. Suleiman M, Jisrawi NM, Dankert O, Reetz MT, Bähtz C, Kirchheim R (2003) Phase transition and lattics expansion during hydrogen loading of nanometer sized palladium clusters. J Alloys Compounds 356/357: 644-648.

31. Robinson IK (2015) Computational studies of hydrogen in palladium. PhD Thesis, University of Salford.

32. Suzana A, Wu L, Assafa T, Williams B, Harder R, Cha W, Kuo C-H, Tsung C-K, Robinson I (2020) Structure of a single nanoparticle and its dynamics during the hydride phase transformation. https://doi.org/10.21203/rs.3.rs-65592/v1 .

33. Houari A, Matar SF, Eyert V (2014) Electronic structure and crystal phase stability of palladium hydrides. J Appl Phys 116: 173706.

34. Briggs D, Seah MP (1990) Practical Surface Analysis, Vol. 1-Auger and X-ray Photoelectron Spectroscopy, 2nd edn. Wiley, Chichester, pp. 613-634 and literature cited therein.

35. Parker SF, Refson K, Hannon AC, Barney ER, Robertson SJ, Albers P (2010) Characterisation of hydrous palladium oxide: Implications for low temperature carbon monoxide oxidation. J Phys Chem C 114: 14164-14171.

36. Albers PW, Möbus K, Wieland SD, Parker SF (2015) The fine structure of Pearlman's catalyst. Phys Chem Chem Phys 17: 5274-5278.

37. Borodziński A, Bond GC (2006) Selective hydrogenation of ethyne in ethene-rich streams on palladium catalysts. Part 1. Effects of changes to catalyst during reaction. Catal Rev 48: 91-144.

38. Parker SF, Bowron DT, Imberti S., Soper AK, Refson K, Lox ES, Lopez M, Albers P (2010) Structure determination of adsorbed hydrogen on a real catalyst. Chem Commun 46: 2959-2961.

39. Loewert M, Serrer M-A, Carambia T, Stehle M, Zimina A, Kalz KF, Lichtenberg H, Saraçi E, Pfeifer P, Grunwaldt JD (2020) Bridging the gap between industry and synchrotron: an operando study at 30 bar over 300 h during Fischer–Tropsch synthesis. React Chem Eng 5: 1071-1082.

40. Davidson AL, Lennon D, Webb PB, Albers PW, Berweiler M, Poss R, Roos M, Reinsdorf A, Wolf D, Parker SF (2021) The characterization of hydrogen on nickel and cobalt catalysts. Topics in Catalysis submitted for publication.

41. Albers P, Angert H, Prescher G, Seibold K, Parker SF (1999) Catalyst poisoning by methyl groups. Chem. Commun. 1619-1620.

42. Albers P, Pietsch J, Parker SF (2001) Poisoning and deactivation of palladium catalysts. J Mol Catal A: General 173: 275-286.

43. Albers PW, Parker SF (2007) Inelastic incoherent neutron scattering in catalysis research. In: Advances in Catalysis, Gates BC, Knözinger H (eds) 51: 99-132.

44. Schulz H (2003) major and minor reactions in Fischer–Tropsch synthesis on cobalt catalysts. Topics in Catalysis 26:73-85.

45. Paul JF, Sautet P (1998) Chemisorption and transformation of CH_x fragments (x=0-3) on a Pd(111) surface: a periodic density functional study. J Phys Chem B 102: 1578-1585.

46. Kellner CS, Bell AT (1981) The kinetics and mechanism of carbon monoxide hydrogenation over alumina supported ruthenium. J Catal 70: 418-432.

Electronic Supplementary Information (ESI)
for:

Applications of Neutron Scattering in Technical Catalysis -

Characterisation of Hydrogenous Species on/in Unsupported and Supported Palladium

Peter W. Albers [a] (ORCID 0000-0001-9564-1713)

and Stewart F. Parker [b] (ORCID 0000-0002-3228-2570)

[a.] Evonik Operations GmbH, Rodenbacher Chaussee 4, D-63457 Hanau-Wolfgang, Germany, (now retired) peterwalbers@web.de

[b.] ISIS Facility, STFC Rutherford Appleton Laboratory, Chilton, Didcot, OX11 0QX, UK, stewart.parker@stfc.ac.uk

Table S1

Summary and References of published examples of activities using neutron scattering techniques for industrial catalysis research at Degussa, Degussa-Hüls, Evonik Industries. 10 – 160 g quantities of technical catalysts and materials of catalytic relevance were investigated per sample with the focus on surface science and bulk characterization via proton dynamics.

Catalyst/application/research target	Result	
C: Carbonaceous catalyst support/final precious metal coated catalyst	Comparison of proton dynamics of commercial activated carbons from different natural resources, carbon blacks, glassy carbon; influence of support on precious metal dispersion over the support's surface and presence as isolated primary particles or aggregates	S1-S4; S5
Pd/C: Hydrogenation catalysts / activated carbon and carbon black supports	Effect of support on average particle size and distribution, hydrogen storage properties, edge decoration of precious metal on carbon black	S2, S3, S5
SiO_2: production of pure silica supports	Fine structures and spectral signature of large quantities of crystalline and amorphous SiO_2	S6, S7
Pearlman's catalyst for C-C-coupling reactions	Identification of fine structure. "$Pd(OH)_2/C$" vs. $C/PdO/OH/H_2O$; hydrous palladium oxide	S8; S9
Pd and Pt: comparison of precious metal blacks and supported catalysts	Surface hydroxyls on fresh prepared catalytic materials and surface states before and after hydrogen treatment	S10, S5
Palladium hydrogenation catalyst: revealing differences in degree of catalyst deactivation of Pd operating in large scale plants over time	Quantitative correlation between degree of activity and increasing deactivation and coverage of catalyst surface with non-extractable molecular entities; "catalyst's surface biography" from precursor species to catalyst poisoning by methyl groups; hydrogen storage inside Pd remained possible at a lower level , adsorption of aromatic molecules onto the surface was hampered/blocked	S11-S15
Coke deposition on catalyst surfaces in low and high temperature processes: Pd/SiO_2 selective cat. hydrogenation of acetylene to ethylene (recycle gas stream in vinyl chloride process); Pt/Al_2O_3 synthesis of hydrogen cyanide from methane and ammonia	Thermally and catalytically driven catalyst coking and catalytic transformation of carbonaceous matter, studied via proton dynamics; feasibility of coke removal, identification of contaminants and their influence in dew point corrosion and macro-, micro-, and nanomorphology of carbonaceous deposits	S16-S19
Pd/C Hydrogenation catalyst, production of stilbenes/Heck reaction, activity and product selectivity, isomer selectivity	Bromobenzene and styrene to stilbenes, strong preferential adsorption of cis-stilbene at catalyst surface, enrichment of trans-stilbene in the organic phase; changes of catalyst support by hydrogen spillover	S20

Pd, Pd/Pt, Pd/Pt/Fe catalysts ("workhorse catalyst") for the hydrogenation of nitrobenzenes to anilines	Influence of particle size and differences in aggregation on hydrogen storage capacity of nanosized entities of precious metal particles (mono-, bi-, trimetallic) in the selective hydrogenation of nitroarenes	S21
Pt/C, Pt black, Hydrogen on platinum	Assignment of occupied surface sites: on-top, twofold, threefold – importance of twofold site, comparison with platinum nanocluster $Pt_{44}H_{80}$	S22
Pt/C and Pt,Ru/C fuel cell catalysts, hydrogen on supported platinum alloy	Catalytic dissociation and adsorption of hydrogen, surface site occupation; impact of different catalyst manufacture on site occupation	S23-S26
Hydrogen storage on/in palladium (metal blacks and supported nanodisperse Pd of different size)	Studies on α- and β-palladium hydride, site occupation, H in on-top position, surface-and subsurface sites and in interstitial occupation, octahedral-sites	S27, S5
Lindlar catalyst, selective hydrogenation of triple bonds to double bonds; e.g. syntheses of vitamins	Influence of lead poisoning/alloying of $Pd/CaCO_3$ on the hydrogen storage properties of finely divided palladium, decrease of β-hydride formation by factor 2	S28
Raney-Nickel / Ni foam, comparison of H on Ni(111) and other surface sites	H on Ni(111); ratio of H on Raney Ni on Ni(111) to H on "non-(111) facets" ca. 5:1 / ratio for H on Ni foam ca. 1:1; Ni foam: more heterogeneous in surfaces-sites	S29
Raney-Cobalt, Co foam and supported Co	Detection of high stability of Co-hydroxyls, detection of H_2 coordinated to Co and H on Co	S30

Table S2
References

Published examples of using neutron scattering techniques for industrial catalysis research by Degussa, Degussa-Hüls, Evonik Industries on large quantities of technical catalysts and materials of catalytic relevance. Tasks from long-term strategic R&D and time critical services in physical chemistry and analytics. Surface science and bulk characterisiation via proton dynamics.

S1. Albers PW, Pietsch J., Krauter J, Parker SF (2003) Investigations of activated carbon catalyst supports from different natural sources. Phys. Chem. Chem. Phys. 5: 1341-49.

S2. Parker SF, Imberti S, Callear SK, Albers PW (2013) The structure of glassy carbon. Chem. Phys. 427: 44-48.

S3. Albers PW, Weber W, Möbus K, Wieland SD, Parker SF (2016) Neutron scattering study of the terminating protons in the basic structural units of non-graphitising and graphitising carbons. Carbon 109: 239-245.

S4. Albers P, Burmeister R, Seibold K, Prescher G, Parker SF, Ross DK (1999) Investigations of palladium catalysts on different carbon supports. J. Catal. 181: 145-154.

S5. Parker SF, Walker HC, Callear SK, Grünewald E, Petzold T, Wolf D, Möbus K, Adam J, Wieland SD, Jiménez-Ruiz M, Albers PW (2019) The effect of particle size, morphology and support on the formation of palladium hydride in commercial catalysts. Chem. Sci. 10: 480-489.

S6. Albers PW, Michael G, Lansink-Rotgerink H, Reisinger M, Parker SF (2012) Low frequency vibrational dynamics of amorphous and crystalline silica. Z. Naturforsch. 67b: 1016-1020.

S7. Parker SF, Klehm U, Albers PW (2020) Differences in the morphology and vibrational dynamics of crystalline, glassy and amorphous silica. Mat. Adv. 1: 749-759.

S8. Albers PW, Möbus K, Wieland SD, Parker SF (2015) The fine structure of Pearlman's catalyst. Phys. Chem. Chem. Phys. 17: 5274-5278.

S9. Parker SF, Refson K, Hannon AC, Barney ER, Robertson SJ, Albers P (2010) Characterisation of hydrous palladium oxide: Implications for low temperature carbon monoxide oxidation. J. Phys. Chem. C 114: 14164-14171.

S10. Parker SF, Adroja D, Jimenez-Ruiz M, Tischer M, Möbus K, Wieland SD, Albers P (2016)
Characterisation of the surface of freshly prepared precious metal catalysts. Phys. Chem. Chem. Phys. 18: 17196-17201; DOI: 10.1039/C6CP01027J.

S11. Albers P, Angert H, Prescher G, Seibold K, Parker SF (1999) Catalyst poisoning by methyl groups. Chem. Commun. No. 17: 1619-1620.

S12. Albers PW, Parker SF Inelastic incoherent neutron scattering in catalysis research (2007). In: Gates BC, Knözinger H (eds) Advances in Catalysis vol. 51 Elsevier, The Netherlands, Amsterdam, 99-132.

S13. Albers P, Pietsch J, Parker SF (2001) Poisoning and deactivation of palladium catalysts
Invited contribution for the special issue "Catalysis with Supported Palladium Metal at the Turn of the 20th Century", Corain B, Kralik M (eds) J. Mol. Catal. A: General 173: 275-286.

S14. Albers PW, Parker SF (2008) Applications of neutron scattering in the chemical industry: proton dynamics of highly dispersed materials, characterization of fuel cell catalysts, and catalysts from large scale chemical processes. In: Neutron Applications in Earth, Energy, and Environmental Services, Liang L, Rinaldi R, Schober H (eds) Springer Science and Business Media, pp. 391- 416.

S15. Albers PW, Lennon D, Parker SF Catalysis (2017). In: Neutron Scattering: Applications in Chemistry, Materials Science, and Biology. In: Fernandez-Alonso F, Price DL (eds) Experimental Methods in the Physical Sciences, Neutron Scattering, vol. 49, Academic Press, USA, Cambridge, pp. 281-350.

S16. Albers P, Seibold K, Prescher G, Müller H (1999) XPS/SIMS-Investigations on carbon species observed on catalysts used in the synthesis of hydrogen cyanide and selective hydrogenation of acetylene. Appl. Catal. A: General 176: 135-146.

S17. Albers P, Prescher G, Seibold K, Parker SF (1999) Applications of neutron scattering for investigating heterogeneous catalysts. Chem. Eng. Technol. CET 22: 135-137.

S18. Albers P, Bösing S, Ross DK, Parker SF (1999) Inelastic neutron scattering investigations of the products of thermally and catalytically driven catalyst coking. Appl. Catal. A: General 187: 233-243.

S19. Albers PW, Bösing S, Ross DK, Parker SF (2002) Inelastic neutron scattering study on the influence of after-treatments on different technical cokes of varying impurity level and sp^2/sp^3 character. Carbon 40: 1449-1558.

S20. Albers PW, Krauter JGE, Ross DK, Heidenreich RG, Köhler K, Parker SF (2004) Identification of surface states on finely divided supported palladium catalysts by means of inelastic incoherent neutron scattering. Langmuir 20: 8254-8260.

S21. Möbus K, Grünewald E, Wieland S, Parker SF, Albers PW (2014) Palladium-catalyzed selective hydrogenation of nitroarenes: influence of platinum and iron on activity, particle morphology and formation of β-palladium hydride. J. Catal. 311: 153-160.

S22. Parker SF, Mukhopadhyay S, Jiménez-Ruiz M, Albers PW (2019) adsorbed states of hydrogen on platinum: A new perspective. Chem. Eur. J. 25: 6496-6499. Chem.201900351.

S23. Albers P, Auer E, Ruth K, Parker SF (2000) Inelastic neutron scattering investigation of the nature of surface sites occupied by hydrogen on highly dispersed platinum on commercial carbon black supports. J. Catal. 196: 174-179.

S24. Albers PW, Lopez M, Sextl G, Jeske G, Parker SF (2004) Inelastic neutron scattering investigation on the site-occupation of atomic hydrogen on platinum particles of different size. J. Catal. 223: 44-53.

S25. Parker SF, Frost CD, Telling M, Albers P, Lopez M, Seitz K (2006) Characterisation of the adsorption sites of hydrogen on Pt/C fuel cell catalysts. Catal. Today 114: 418-421.

S26. Albers PW, Weber W, Kunzmann K, Lopez M, Parker SF (2008) Characterization of carbon supported platinum-ruthenium fuel cell catalysts of different degree of alloying. Surf. Sci. 602: 3611-3616.

S27. Albers P, Poniatowski M, Parker SF, Ross DK (2000) Inelastic neutron scattering study on different grades of palladium of varying pretreatment. J. Phys.: Condens. Matter 12: 4451-4463.

S28. Albers PW, Möbus K, Frost CD, Parker SF (2011) Characterisation of beta palladium hydride formation in the Lindlar catalyst and on carbon supported palladium. J. Phys. Chem. C 115: 24485-24493.

S29. Parker SF, Bowron DT, Imberti S, Soper AK, Refson K, Lox ES, Lopez M, Albers P (2010) Structure determination of adsorbed hydrogen on a real catalyst. Chem. Commun. 46: 2959-2961.

S30. Davidson AL, Lennon D, Webb PB, Albers PW, Berweiler M, Poss R, Roos M, Reinsdorf A, Wolf D, Parker SF (2021) The characterization of hydrogen on nickel and cobalt catalysts. Topics in Catalysis, accepted for publication